RESEARCH ARTICLE

Human Mutation

OFFICIAL JOURNAL
HGVS
HUMAN GENOME VARIATION SOCIETY
www.hgvs.org

In Vitro Correction of a Pseudoexon-Generating Deep Intronic Mutation in LGMD2A by Antisense Oligonucleotides and Modified Small Nuclear RNAs

Lorea Blázquez,[1,2]* Ana Aiastui,[2,3] Maria Goicoechea,[2,3] Mafalda Martins de Araujo,[4] Aurélie Avril,[5] Cyriaque Beley,[5] Luis García,[5] Juan Valcárcel,[4] Puri Fortes,[1]† and Adolfo López de Munain[2,3,6,7]†

[1] *Center for Applied Medical Research (CIMA), University of Navarra, Pamplona, Spain;* [2] *Neuroscience Area, Health Research Institute Biodonostia, San Sebastian, Spain;* [3] *CIBERNED, Carlos III Institute, Ministry of Economy and Competitiveness, Madrid, Spain;* [4] *Center for Genomic Regulation (CRG), Barcelona, Spain;* [5] *Université Pierre et Marie Curie, Paris, France;* [6] *Neurology Department, Donostia University Hospital, San Sebastián, Spain;* [7] *Department of Neurosciences, University of the Basque Country, San Sebastián, Spain*

Communicated by Jacques S. Beckmann

Received 16 January 2013; accepted revised manuscript 8 July 2013.
Published online 17 July 2013 in Wiley Online Library (www.wiley.com/humanmutation). DOI: 10.1002/humu.22379

ABSTRACT: Limb-girdle muscular dystrophy type 2A (LGMD2A) is the most frequent autosomal recessive muscular dystrophy. It is caused by mutations in the calpain-3 (*CAPN3*) gene. The majority of the mutations described to date are located in the coding sequence of the gene. However, it is estimated that 25% of the mutations are present at exon–intron boundaries and modify the pre-mRNA splicing of the *CAPN3* transcript. We have previously described the first deep intronic mutation in the *CAPN3* gene: c.1782+1072G>C mutation. This mutation causes the pseudoexonization of an intronic sequence of the *CAPN3* gene in the mature mRNA. In the present work, we show that the point mutation generates the inclusion of the pseudoexon in the mRNA using a minigene assay. In search of a treatment that restores normal splicing, splicing modulation was induced by RNA-based strategies, which included antisense oligonucleotides and modified small-nuclear RNAs. The best effect was observed with antisense sequences, which induced pseudoexon skipping in both HeLa cells cotransfected with mutant minigene and in fibroblasts from patients. Finally, transfection of antisense sequences and siRNA downregulation of serine/arginine-rich splicing factor 1 (SRSF1) indicate that binding of this factor to splicing enhancer sequences is involved in pseudoexon activation.

Hum Mutat 34:1387–1395, 2013. © 2013 Wiley Periodicals, Inc.

KEY WORDS: limb-girdle muscular dystrophy; LGMD2A; pseudoexon; exon skipping; antisense oligonucleotide; AON; usnRNA

Introduction

Limb-girdle muscular dystrophy type 2A (LGMD2A; MIM #253600) is an autosomal recessive disorder caused by mutations in the *CAPN3* gene (MIM #114240, GenBank NM_000070.2), which codes for the muscle-specific calcium-dependent cysteine protease calpain 3 [Richard et al., 1995]. Patients with LGMD2A show a progressive degeneration of scapular and pelvic musculature, whereas facial muscles are preserved [Fardeau et al., 1996; Urtasun et al., 1998]. Calpain 3 was initially described in 1989 [Sorimachi et al., 1989]. However, its function is somewhat unknown. While calpain 3 is a proteolytic enzyme, it is estimated that one-third of LGMD2A biopsies exhibit a near-normal level of calpain 3 proteolytic activity [Milic et al., 2007]. Moreover, mutations that do not affect calpain 3 proteolytic activity but nevertheless cause muscular dystrophy have been described [Ermolova et al., 2011]. Therefore, it has been proposed that calpain 3 plays a structural function in the cellular compartments where it is localized and that this function is impaired in calpain 3-deficient muscle [Kramerova et al., 2008; 2012; Ojima et al., 2011].

To date more than 450 different pathogenic mutations in the *CAPN3* gene have been identified, the majority of which are located in the coding region of the gene and represent nonsynonymous amino-acid substitutions (www.dmd.nl/capn3). However, it is estimated that 25% of the mutations are synonymous substitutions as well as deletions and insertions located at intron–exon boundaries that act by modifying precursor mRNA (pre-mRNA) splicing [Blazquez et al., 2008; Krahn et al., 2007]. For the experimental demonstration of the pathogenicity of these mutations, it is necessary to analyze the *CAPN3* mRNA to determine whether there is aberrant splicing induced by these alterations [Krahn et al., 2007; Nascimbeni et al., 2010]. However, muscle tissue from muscle biopsies is limited and not always available for molecular studies. Although initially described as muscle specific, *CAPN3* mRNA is detected in tissues other than muscle [De Tullio et al., 2003]. Based

Additional Supporting Information may be found in the online version of this article.

†These authors contributed equally to this work.

*Correspondence to: Lorea Blázquez, Department of Gene Therapy and Hepatology, Center for Applied Medical Research (CIMA), University of Navarra, Avda. Pio XII, 55, Pamplona 31008, Spain. E-mail: lblazquez@unav.es

Contract grant sponsors: Spanish Ministry of Health (FIS PI06/1018, FIS PI09-116, PS09-00660); Spanish Ministry of Science and Innovation (BIO2006-13225, BIO 2009/09295, RNAREG CSD2009-00080, PTQ-09-02-02213); Ilundain Foundation; Isabel Gemio Foundation; Diputación Foral de Guipuzcoa (DFG09/001); Association Française contre les Myopathies (Ref. 12642); UTE project CIMA and Department of Education, University and Research of the Basque Government.

on this work, we have previously characterized splice-site mutations in LGMD2A patients sequencing the *CAPN3* transcripts from peripheral blood [Blazquez et al., 2008]. This procedure allowed the identification of splicing alterations induced by seven splice-site mutations in the *CAPN3* gene. Among the splice-site mutations identified, we described the first deep intronic mutation in the *CAPN3* gene: c.1782+1072G>C mutation. This mutation, identified in 6 LGMD2A families to date, consists of a G to C transversion at +1072 position of intron 14 that causes the insertion of 100 bp of intron 14 in mature mRNA. The new transcript breaks the reading frame and leads to a truncated protein due to the presence of a stop codon 69 amino acids later. In the presence of the mutation, a new acceptor splice site within intron 14 with an increased splice-site score might cause the exonization of the intronic sequence. However, no experimental confirmation that the mutation induced the pseudoexonization was obtained at that time. The definition of an exon is regulated by the presence of many splicing regulatory elements in the pre-mRNA. It includes conserved sequences at the 5′ss and 3′ss, but also other *cis*-acting pre-mRNA elements named exonic and intronic splicing enhancers (ESEs and ISEs) or silencers (ESSs and ISSs). These sequences are typically short and diverse in sequence and modulate both constitutive and alternative splicing by binding regulatory proteins that either stimulate or repress the assembly of spliceosomal complexes at an adjacent splice site [Will and Luhrmann, 2011].

In recent years, mRNA analysis has allowed the identification of several pseudoexon-generating deep intronic mutations in many disease-associated genes [Dehainault et al., 2007; Homolova et al., 2010; Spier et al., 2012]. When such mutations are the drivers of the disease, a promising therapeutic approach is the use of molecules that correct pre-mRNA splicing by splicing modulation. These strategies have led to encouraging results in several disorders. In most cases, the molecules used for splicing modulation are antisense oligonucleotides (AONs) [Friedman et al., 1999; Hua et al., 2010; 2011; Mancini et al., 2012; Rodriguez-Pascau et al., 2009; van Deutekom et al., 2001; Wein et al., 2010]. However, antisense sequences can also be part of modified uridine-rich small-nuclear RNAs (U snRNAs). U7 and U1 snRNA-derived antisense molecules have been shown to be effective in inducing exon skipping. U7 snRNA is normally involved in histone pre-mRNA 3′-end processing, but can be converted into a versatile tool for splicing modulation by a small change in the binding site for Sm/Lsm proteins [Schumperli and Pillai, 2004]. Thus, modified U7 snRNAs have been used to correct splicing defects [Brun et al., 2003; Gedicke-Hornung et al., 2013; Goyenvalle et al., 2004; Meyer et al., 2009; Vulin et al., 2012]. U1 snRNA, together with other U snRNAs, is part of the spliceosome, which catalyzes pre-mRNA splicing. U1 snRNA specifically base pair to the 5′ splice site (5′ss) of pre-mRNA at the earliest stage of spliceosome assembly [Black, 2003]. U1 snRNAs can be modified to induce gene silencing [Blazquez et al., 2012; Fortes et al., 2003], to increase complementarity to mutated 5′ss [Fernandez Alanis et al., 2012; Pinotti et al., 2008; Schmid et al., 2011; Tanner et al., 2009] and to deliver antisense sequences that induce exon skipping/inclusion [Cazzella et al., 2012; Denti et al., 2006; Incitti et al., 2010]. In modified U snRNAs, the antisense sequence is embedded into a snRNP particle where it is protected from degradation and accumulates in the nucleus where splicing occurs.

In the present work, we experimentally confirm that c.1782+1072G>C mutation increases the pseudoexonization of 100 bp of intron 14 in the *CAPN3* mRNA using a minigene assay. Moreover, splicing modulation was induced to restore the correct reading frame of the *CAPN3* transcript by using AONs and modified U7 and U1-snRNAs. Although full details of the molecular mechanism that explains pseudoexon recognition remain to be discovered, siRNA experiments and delivery of antisense sequences suggest that SRSF1 binding to exonic splicing enhancers (ESE) in the pseudoexon favor pseudoexon recognition.

Materials and Methods

Patients and Controls

LGMD2A patient is a 48-year-old woman suffering from muscular dystrophy since she was 13 and wheelchair bound for the last 18 years. She presented a clinical and radiological phenotype compatible with LGMD2A, but only a c.2362_2363delinsTCATCT mutation in heterozygosis was identified after DNA analysis of the coding sequence of the *CAPN3* gene. The second mutation, named c.1782+1072G>C, was described in a previous study [Blazquez et al., 2008] after sequencing the *CAPN3* transcript present in white blood cells. Mutations are numbered based on cDNA sequence (GenBank Reference Sequence NM_000070.2) according to guidelines (www.hgvs.org/mutnomen). Nucleotide 1 is the A of the ATG-translation initiation codon. Skin biopsy from LGMD2A patient was obtained in the Neurology Department of Donostia University Hospital. The skin biopsy was stored in RPMI medium in the presence of 2% penicillin/streptomycin at room temperature and immediately processed for fibroblast isolation. The ethics committee of Donostia University Hospital approved the experiment. Informed consent was obtained before the initiation of the experiment.

Cell Lines

For the isolation of primary fibroblasts, skin was chopped into 2–3 mm^3 fragments and placed on a surface moistened with modified Eagle's medium containing 13% newborn calf serum, 0.4 % penicillin/streptomycin, and 2 mM L-glutamine. The flasks were incubated vertically for 3–6 H at 37°C with 5 % CO_2 and returned to the horizontal position. Human fibroblasts were cultured in Dulbecco's Modified Eagle Medium (DMEM), containing 10 % FBS and 1% penicillin–streptomycin.

The HeLa cell line was obtained from the American Type Culture Collection (ATCC Number CCL-2). Cells were cultured in DMEM, supplemented with 10% FBS and 1% penicillin–streptomycin, at 37°C in a 5% CO_2 atmosphere. All cell culture reagents were obtained from Gibco BRL/Life Technologies (CA, USA).

RNA Analysis

Total RNA was isolated from cell samples using TRI-Reagent following the manufacturer's instructions (Sigma–Aldrich, St. Louis, MO, USA). Total RNA was DNAse I treated (Fermentas, Vilnius, Lithuania) and reverse-transcribed with MMLV reverse transcriptase (Promega, Madison, WI, USA).

Minigene Construction and In Vitro Splicing Analysis

For minigene construction, a DNA fragment that contained exon 14, intron 14, and exon 15 of the *CAPN3* gene was amplified from the genomic DNA of the patient using the oligonucleotides Minigene-Fw (5′CGAGGTACCGGAAGTTGAAAATACC 3′) and Minigene-Rv (5′AGCAGCGGCCGCCCACACACCTACCTTGG 3′). The oligonucleotides included restriction sites for *Asp*718 (Roche

Roche Diagnostics, Mannheim, Germany) and *Not*I (New England Biolabs, Hitchin, UK) enzymes, respectively. The PCR product was digested and ligated into the *Asp*718–*Not*I site of pCMVΔβgal vector, under CMV promoter. As the patient is heterozygous for the c.1782+1072G>C and c.2362_2363delinsTCATCT mutation, which is located in exon 22, mutant and wild-type minigenes with or without the deep intronic mutation respectively were isolated from different clones.

For the in vitro splicing evaluation of minigene constructs, 1 μg of the wild-type or mutant minigenes was transfected into 4×10^5 HeLa cells, grown in six-well plates, with 6 μl of Lipofectamine 2000 Reagent (Life Technologies). Total RNA was isolated from cultured cells 24 H after transfection. RNA was reverse transcribed to first-strand complementary DNA (cDNA) using the pCMVΔβgal specific 4348 reverse primer (5′ GTGGTTTGTCCAAACTCATCAA 3′) to avoid retrotranscription of endogenous *CAPN3* mRNA. PCR amplification was performed using Minigene Fw and pCMV4348 reverse primer in a PCR reaction of 25 cycles.

In Silico Analyses of Intronic Sequence

Predictive programs ESE Finder 3.0 (http://rulai.cshl.edu/tools/ESE/) [Cartegni et al., 2003; Smith et al., 2006], ESR Search (http://esrsearch.tau.ac.il/) [Goren et al., 2006], Human Splicing Finder (http://www.umd.be/HSF/) [Desmet et al., 2009], and Alternative Splicing Database-Splicing Rainbow (http://www.ebi.ac.uk/asd-srv/wb.cgi) [Stamm et al., 2006] were used for the identification of exonic and intronic splicing regulatory sequences.

Splice scores of wild-type and cryptic donor and acceptor sites were calculated in the Splice Site Score Calculation Website (http://rulai.cshl.edu/new_alt_exon_db2/HTML/score.html).

Treatment with AONs and In Vitro Splicing Analysis

AONs with full-length 2′-*O*-methyl-substituted ribose moieties and phosphorothioate internucleotide linkages were purchased from Sigma Proligo. Sequences of AONs complementary to acceptor splice site (SA AON), donor splice site (SD AON), SRSF1 binding site (SRSF1 AON), or control AON were: 5′ ACCUACCAGUAAAAC CAAUC 3′, 5′ CUCUACUCACGUGACGUGCC 3′, 5′ ACACCGAU GACCAGCAUCCA 3′, and 5′ AUGCUUUCCUCUCCACAAUG 3′, respectively. 4×10^5 HeLa cells or fibroblasts, grown in six-well plates, were transfected at a final concentration of 200 nM with 6 μl of Lipofectamine 2000 Reagent (Life Technologies). Total RNA was isolated from cultured cells 24 H after transfection. In HeLa cells, total RNA and RT-PCR analysis was performed as described above. In fibroblasts, RNA was reverse transcribed to first-strand cDNA using Random Primers. PCR amplification was performed using CAPN3×13Fw (5′ ATTCATCCTCCGGGTCTTCT 3′) and CAPN3×16Rv (5′ TCCTCTGACTCCTGGTCCA C 3′) primers in a PCR reaction of 35 cycles.

Treatment with Modified U snRNAs and In Vitro Splicing Analysis

pGEM-U1αCAPN3 constructs, expressing modified U1 snRNAs that target 2 different regions of pseudoexon boundaries in the *CAPN3* pre-mRNA, were cloned by ligation of base paired oligonucleotides with antisense sequences for *CAPN3* into the *Nco*I/*Bcl*I site of pGEM-U1inWt. pGEM-U1inWt plasmid was used as control. In pGEM-U1inWt construct, U1 snRNA sequence along with its natural promoter and 3′ sequences is cloned. The U1snRNA gene expressed from this plasmid contains four point mutations to distinguish it from the endogenous U1snRNA, but it is identical in functionality to endogenous U1-snRNA [Blazquez et al., 2012]. Antisense sequences to SA and SD sites cloned in pGEM-U1αCAPN3 constructs were 5′ CACACACCTACCAGTAAAAC 3′ and 5′ CTCTACTCACGTGACGTGCC 3′, respectively.

pGEM-U7αCAPN3 construct, expressing human-modified U7 gene along with its natural promoter and 3′ elements, was constructed by cross-over PCR using pSMD2-SU7OptDtex23 plasmid as template [Goyenvalle et al., 2004] and oligonucleotides that included sequences complementary to pseudoexon splice-donor sequence. To construct pGEM-U7αCtrl construct, the modified U7 gene complementary to mouse dystrophin (*DMD*) gene was amplified from pSMD2-SU7OptDtex23 plasmid. PCR products were subsequently cloned into pGEM-T Easy vector (Promega, Madison, WI, USA). Antisense sequence to SD site cloned in pGEM-U7αCAPN3 construct was: 5′ CACCTGCCTGCTCTACTCACGT-GACGTGCCAGCTCCCATA 3′.

For the analysis of splicing modulation by modified snRNAs, 0.5 μg of the mutant minigene was cotransfected with 0.5 μg of pRL-SV40 plasmid (Promega, Madison, WI, USA) and 3 μg of pGEM-U7αCAPN3, pGEM-U1αCAPN3 or control constructs into 4×10^5 HeLa cells, grown in six-well plates, with 6 μl of Lipofectamine 2000 Reagent (Life Technologies). pRL-SV40 plasmid, which expresses Renilla luciferase, was used as a transfection control. Total RNA and RT-PCR analysis was performed as described above. To quantify the expression of modified U7 and U1 snRNAs, 1 μg of total RNA was reverse transcribed with random primers. snRNA expression was measured by quantitative real-time PCR (qRT-PCR) with primers designed to detect modified U7-snRNAs (U7-SD-Fw: 5′ ACCTGCCTGCTC TACTCACG 3′, U7-dmd-Fw: 5′ CCAAACCTCGGCTTACCTAAA 3′, U7-Rv: 5′ GCCAGAAAGCCTACTCCAAA 3′), U1-snRNAs (U1-Fw: 5′ TGGCAGG GGAGATACCAT 3′, U1-Exo-Rv: 5′ CGAGTTTG GCACATTTGGCC 3′), and Renilla luciferase mRNA (SV-RL Fw: 5′ GCAAATCAGGCAAATCTGGT 3′, SV-RL Rv: 5′ CCATTCATC CCATGATTCAA 3′).

RNA Interference

For RNA interference, 4×10^5 HeLa cells, grown in six-well plates were transfected with mock, control siRNA (5′ CCUGACU UGUAAACUGUGA 3′) or SRSF1 siRNA (5′ ACGAUUGCCGCAU CUACGU 3′) at a final concentration of 40 nM with 6 μl of Lipofectamine 2000 Reagent (Life Technologies). Forty-eight hours later the cells were transfected with 1 μg of the wild-type or mutant minigenes with calcium phosphate as described elsewhere [Blazquez et al., 2012]. Cells were harvested 72 H after the initial siRNA transfection and splicing evaluation of minigene constructs was performed as described above. SRSF1 downregulation was monitored by Western blotting using an SRSF1 mouse monoclonal antibody (mAb96; Invitrogen, Carlsbad (CA), USA). β-actin expression was quantified with anti β-actin antibody (A2066; Sigma). Quantification of PCR and WB bands was performed using NIH ImageJ software.

Statistical Analysis

Data are expressed as mean ± standard deviation (SD). Statistical analysis was performed with Kruskal–Wallis test using the GraphPad Prism Software. Statistically significant differences ($P < 0.05$) are indicated with a star.

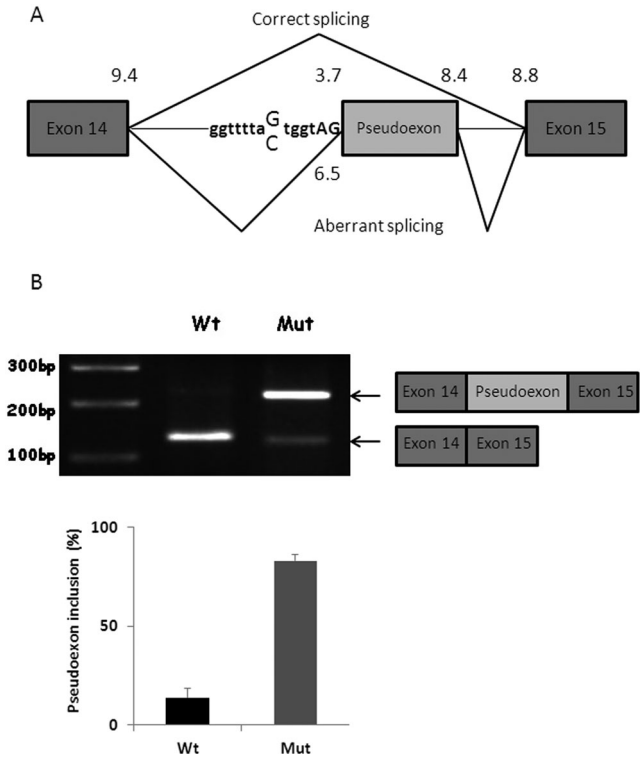

Figure 1. Recognition of the *CAPN3* pseudoexon is dependent on the presence of the c.1782+1072G>C mutation. **A:** Scheme of part of the *CAPN3* gene that contains the c.1782+1072G>C mutation, showing the pseudoexon included in patients. Numbers indicate the scores for the corresponding 5′ and 3′ splice sites. Note that the mean score of a 3′ss and a 5′ss in constitutive exons is 7.9 and 8.1, respectively. **B:** Splicing minigene assay. Wild-type (Wt) or mutant (Mut) minigenes were transiently transfected in HeLa cells. After RNA isolation the splicing products were analyzed by RT-PCR using minigene-specific primers. The upper panel shows agarose gel electrophoresis. The lower band represents correctly spliced exons, whereas the upper band represents *CAPN3* pseudoexon inserted between minigene exons. The lower panel shows the average of pseudoexon inclusion levels in three independent experiments. Quantification of PCR bands was performed using NIH ImageJ software.

Results

In Vitro Expression of a Minigene Containing c.1782+1072G>C Mutation

In a previous study, the analysis of the *CAPN3* transcript present in white blood cells identified a truncated isoform of *CAPN3* mRNA in five patients in whom only one mutation in the *CAPN3* gene had been previously identified [Blazquez et al., 2008]. The truncated isoform contained 100 bp of intron 14 in the mature mRNA. These patients had a G to C transversion at 1072 position of intron 14 that was not present in 100 control chromosomes. In addition, this nucleotide change increased the score of the pseudoexon cryptic 3′ss from 3.7 to 6.5 (the mean score of a 3′ss in constitutive exons is 7.9) (Fig. 1A). Therefore, we proposed that the c.1782+1072G>C mutation could induce the pseudoexonization of 100 bp of intron 14 in the *CAPN3* mRNA (Fig. 1A). To provide evidence that the change causes pseudoexon inclusion in patients' mRNA, we designed a minigene assay. The *CAPN3* exon 14, intron 14, and exon 15 from the wild-type or mutant allele were cloned in the pCMV$\Delta\beta$gal plasmid. Figure 1B shows the result of the splicing analysis after transfection of either wild-type or mutant minigenes in HeLa cells. Transfection of wild-type minigene resulted in 13.7 ± 4.9% of mRNAs including the pseudoexon, whereas 82.9 ± 3.4% of mRNAs included the pseudoexon when mutant minigene was transfected (Fig. 1B). Sequencing of PCR products confirmed that the upper band contained the pseudoexon, whereas in the lower band, correct fusion between exons 14 and 15 had occurred (data not shown). Therefore, we confirmed that the c.1782+1072G>C mutation affects normal splicing and can be considered pathogenic.

In Silico Modification of Splicing Regulatory Sequences by c.1782+1072G>C Mutation

The pseudoexonized sequence and its 5′ and 3′ss with or without the mutation were scanned for splicing regulatory sequences using the predictive programs described in Materials and Methods. In silico analysis using ESE Finder and Human Splicing Finder predicts a binding site for splicing-component 35 kDa (SC35) in the presence of the mutation (TTTTA**C**TG). Furthermore, the mutation may increase the binding score of a serine-arginine protein 40 (SRp40) motif (TTA**C**TGG) according to all programs. Human Splicing Finder program predicts a heterogeneous ribonucleoprotein A1 (hnRNPA1) binding site (TA**G**TGG) that was predictably affected by the presence of the mutation (Supp. Fig. S1). Several binding sequences for SRSF1 splicing factor were identified in the proximity of the mutation. However, none of them was disrupted by the presence of the mutation.

Splicing Modulation by AONs

As the mutation may modify the binding of several splicing regulatory proteins, we designed an AON complementary to cryptic acceptor ss (SA AON) in order to block the access of the splicing machinery and avoid the inclusion of pseudoexon in the *CAPN3* pre-mRNA (Supp. Fig. S1). Furthermore, we designed an AON complementary to donor ss (SD AON) to analyze if an accessible 5′ss was also necessary for efficient pseudoexon recognition. HeLa cells were cotransfected with mutant *CAPN3* minigene and either SA, SD or Ctrl AONs. Cells were harvested 24 H after transfection and splicing was analyzed by RT-PCR using oligonucleotides complementary to sequences in the vector part of the minigene, to avoid amplification of endogenous *CAPN3*. The results indicate that SD AON was able to rescue correct splicing almost completely, whereas SA AON only induced pseudoexon skipping in 24.4% of pre-mRNAs (Fig. 2). The effect of the oligonucleotide treatment was sequence specific because a nonspecific Ctrl AON did not prevent pseudoexon inclusion. Splicing of wild-type minigene was not affected by AON treatment either (Supp. Fig. S2).

Splicing Modulation Induced by Modified U-snRNAs

We next designed modified U-snRNAs to compare the efficiency of exon-skipping between AONs and modified U-snRNAs. One U7-snRNA construct and two U1-snRNA constructs that bear antisense sequences toward different regions of pseudoexon boundaries were cloned. The 5′ end region of U7-snRNA, which functions as a natural antisense sequence by hybridizing with the 3′ end of histone pre-mRNA, was replaced by a 40 nucleotide-long sequence complementary to the donor site in pseudoexon 5′ss, giving rise to the U7αCAPN3-SD construct. In U1 constructs, U1-snRNA nucleotides 2-11 nucleotides, that are used in 5′ss recognition, were

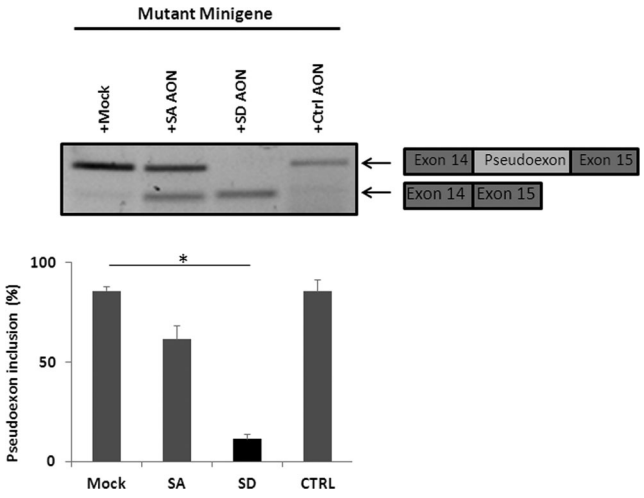

Figure 2. Antisense oligonucleotide (AON) treatment in HeLa cells cotransfected with mutant minigene. HeLa cells were cotransfected with mutant minigene (Mock) and AONs that target splice acceptor site (SA), splice donor site (SD), or an irrelevant sequence (Ctrl). The upper panel shows agarose gel electrophoresis of the RT-PCR amplification of RNA extracted from cells 24 H posttransfection using minigene-specific primers. The lower panel shows the average of pseudoexon inclusion levels in three independent experiments. Quantification of PCR bands was performed using NIH ImageJ software.

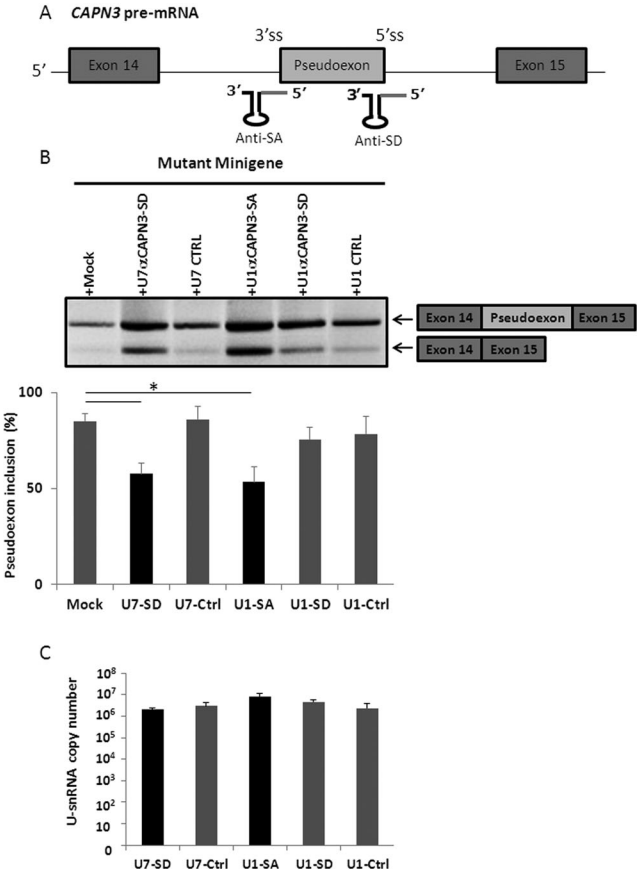

Figure 3. Modified U-snRNA treatment in HeLa cells cotransfected with mutant minigene. **A:** Scheme of the *CAPN3* pre-mRNA fragment that contains pseudoexon. Modified U-snRNAs that target splicing acceptor sites (3′ss) and splicing donor sites (5′ss) are represented below. **B:** HeLa cells were cotransfected with mutant minigene (Mock) and plasmids that express modified U7-snRNAs or U1-snRNAs. The 5′ extreme of U-snRNAs is modified to target pseudoexon splicing acceptor site (SA), splicing donor site (SD), or irrelevant sequences (Ctrl). The upper panel shows agarose gel electrophoresis of the RT-PCR amplification of RNA extracted from cells 24 H posttransfection using minigene-specific primers. The lower panel shows the average of pseudoexon inclusion levels in three independent experiments. Quantification of PCR bands was performed using NIH ImageJ software. **C:** Quantification of modified U-snRNAs expression level in three independent experiments. Total RNA of HeLa cells transfected with plasmids that express modified U-snRNAs was reverse transcribed with random primers. U-snRNA copy number was quantified by qRT-PCR using oligonucleotides designed to amplify exogenous U-snRNAs. The copy number of U-snRNAs was corrected in each case for transfection efficiency by Renilla luciferase mRNA copy number.

replaced by 20 nucleotide-long antisense sequences complementary to the acceptor site in pseudoexon 3′ss or the donor site in pseudoexon 5′ss, giving rise to U1αCAPN3-SA or U1αCAPN3-SD constructs, respectively (Fig. 3A).

HeLa cells were cotransfected with mutant *CAPN3* minigene construct and plasmids that express U1 or U7 snRNAs complementary to pseudoexon boundaries (U7αCAPN3-SD, U1αCAPN3-SA, and U1αCAPN3-SD) or unrelated sequences (U7-Ctrl and U1-Ctrl). Figure 3B shows RT-PCR performed with a forward primer located in exon 14 (Minigene-Fw) and a reverse primer located in an internal portion of the minigene plasmid (pCMV4348R). The results show that when the mutant minigene was cotransfected with U7αCAPN3-SD or U1αCAPN3-SA constructs, pseudoexon skipping was induced in more than 25% of pre-mRNAs expressed from mutant minigene plasmid. In contrast, neither U1αCAPN3-SD construct nor control constructs induced a statistically significant decrease of pseudoexon inclusion. Likewise, cotransfection of wild-type construct with plasmids that express modified U-snRNAs did not affect pseudoexon inclusion level (Supp. Fig. S2).

Quantification of U1 and U7 snRNAs by qRT-PCR determined that all U-snRNAs, including control U-snRNAs were expressed at similar levels (Fig. 3C). The copy number of U-snRNAs was normalized in each case for transfection efficiency by Renilla luciferase mRNA copy number.

SRSF1 Regulates Pseudoexon Inclusion

Contrary to what we initially expected, SA-AON, which masks the acceptor site where mutation is located, only decreased pseudoexon inclusion levels in 24.4% of pre-mRNA molecules expressed from mutant minigene (Fig. 2). In contrast, SD-AON, which masks the donor site, induced pseudoexon skipping to wild-type minigene levels (Fig. 1B and 2). In silico analysis of the sequences recognized by both AONs with predictive programs that identify exonic and intronic splicing elements predicted that SD-AON masks two overlapping very strong SRSF1 binding motifs (scores higher than 3.5 according to ESE finder) (Fig. 4A). To answer whether other SRSF1 binding sites also favor pseudoexon recognition, an additional AON that masks an internal putative SRSF1 binding site was designed (SRSF1 AON) (Fig. 4A). As observed in Figure 4B, HeLa cells cotransfected with mutant *CAPN3* minigene and SRSF1 AON showed decreased pseudoexon inclusion levels, similar to those obtained with SD AON. On the contrary, pseudoexon-inclusion level was not modified when SRSF1 AON was cotransfected with wild-type minigene (Supp. Fig. S2, lane 4).

Furthermore, we analyzed if downregulation of SRSF1 had any effect on pseudoexon inclusion. Transfection of HeLa cells with a

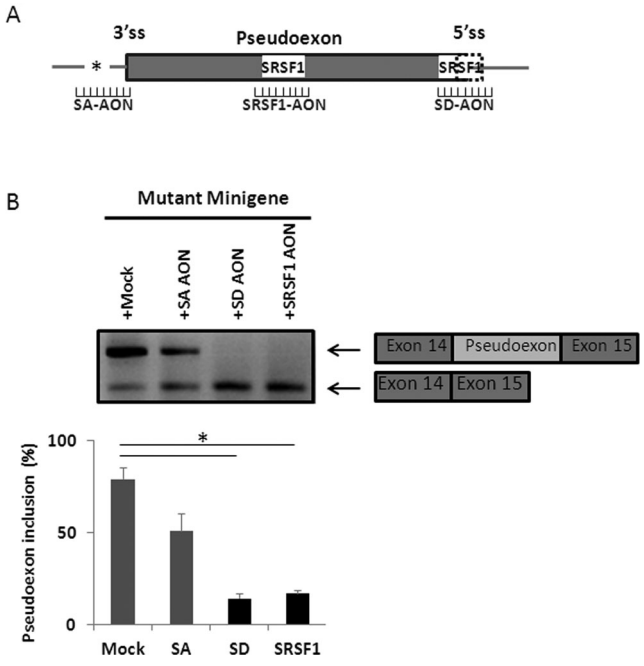

Figure 4. SRSF1 regulates *CAPN3* pseudoexon inclusion. **A:** Scheme of the pseudoexon containing pre-mRNA fragment. Pseudoexon is depicted as a grey box. Putative SRSF1 binding sites are shown inside as white boxes. AONs and the sequences recognized by them are represented below. The position of the pseudoexon-generating mutation is indicated with an asterisk. **B:** HeLa cells were cotransfected with mutant minigene (Mock) and AONs that target splice acceptor site (SA), splice donor site (SD), or other SRSF1 putative binding site in the pseudoexon (SRSF1). The upper panel shows agarose gel electrophoresis of the RT-PCR amplification of RNA extracted from cells 24 H posttransfection using minigene-specific primers. The lower panel shows the average of pseudoexon inclusion levels in three independent experiments. Quantification of PCR bands was performed using NIH ImageJ software.

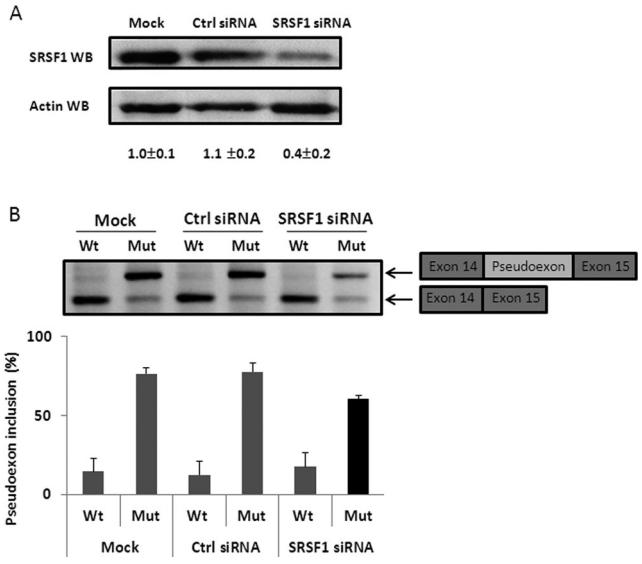

Figure 5. Down-regulation of SRSF1 induced pseudoexon skipping. HeLa cells were transfected with double-stranded RNA oligonucleotides directed toward the SRSF1 mRNA or a negative control. Forty eight hours after siRNA transfection *CAPN3* wild-type (Wt) or mutant (Mut) minigenes were transfected. Cells were harvested 24 H later. **A:** SRSF1 downregulation by Western blotting. Quantification of SRSF1 protein expression level was corrected in each case by β-actin protein level. The average of SRSF1 expression level in two independent experiments is indicated below. Quantification of WB bands was performed using NIH ImageJ software. **B:** The upper panel shows agarose gel electrophoresis of the RT-PCR amplification of RNA extracted from cells using minigene-specific primers. The lower panel shows the average of pseudoexon inclusion levels in two independent experiments. Quantification of PCR bands was performed using NIH ImageJ software.

siRNA designed to downregulate SRSF1 decreased cellular amounts of SRSF1 to 40% (Fig. 5A). This decrease correlated with a reduction in pseudoexon inclusion levels in cells transfected with mutant *CAPN3* minigene. However, decreased levels of SRSF1 did not modify the splicing pattern of wild-type *CAPN3* minigene (Fig. 5B). The splicing of the minigene was not modified either when a control siRNA was transfected in HeLa cells before wild-type or mutant *CAPN3* minigene transfection, indicating that the decrease in pseudoexon inclusion observed when the cellular amounts of SRSF1 are downregulated is specific (Fig. 5B).

AON Treatment of Patient's Fibroblasts

To analyze if AON treatment can induce pseudoexon skipping in endogenous *CAPN3* mRNA, fibroblasts from an LGMD2A patient were subsequently treated with AONs. Human fibroblasts express two different *CAPN3* isoforms that differ in the presence or absence of exon 6 (data not shown). LGMD2A fibroblasts were transfected with SA, SD, SRSF1, or control AONs and cells were harvested 24 H after transfection. Splicing modulation was analyzed by RT-PCR using oligonucleotides that amplify endogenous *CAPN3*. LGMD2A patient is a compound heterozygous and contains different mutations in each *CAPN3* allele. Therefore, two different PCR products that contain or not pseudoexon are amplified in nontreated cells. As observed in Figure 6, SA AON transfection did not result in a

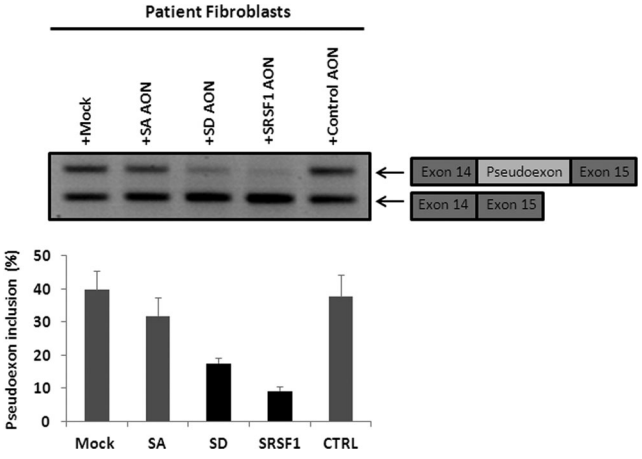

Figure 6. AON treatment in patient's fibroblasts. Fibroblasts from an LGMD2A patient heterozygous for c.1782+1072G>C mutation were transfected with AONs that target splice acceptor site (SA), splice donor site (SD), other SRSF1 putative binding sites in pseudoexon (SRSF1) or an irrelevant sequence (Ctrl). The upper panel shows agarose gel electrophoresis of the RT-PCR amplification of RNA extracted from cells 24 H after transfection using oligonucleotides that amplify endogenous *CAPN3* mRNA. The upper band contains pseudoexon and is expressed from the allele that contains c.1782+1072G>C mutation. The lower band represents correctly spliced mRNA. It is expressed from the allele that does not contain the deep-intronic mutation or from corrected *CAPN3* pre-mRNAs after AON treatment. The lower panel shows the average of pseudoexon inclusion levels in two independent experiments.

relevant decrease in pseudoexon inclusion. On the contrary, cells transfected with SD or SRSF1 AONs showed a decrease in the abnormally spliced mRNA, indicating a correction in favor of normal splicing. Again, the effect of the AON treatment was sequence specific because control AON did not induce pseudoexon skipping.

Discussion

In the present study, we demonstrate that c.1782+1072G>C is a pseudoexon generating deep intronic mutation in the *CAPN3* gene (Fig. 1). The mutation is located in the polypyrimidine tract (PPT) that precedes the conserved AG dinucleotide at the 3′ end of an intron. This modification triggers 3′ss recognition, and consequently pseudoexon inclusion, but not through the classical interactions leading to PPT and branch point activation, as in vitro recruitment of U2 auxiliary factor 65 ($U2AF^{65}$) or U2 small nuclear ribonucleoprotein (U2-snRNP) to pseudoexon 3′ss was not modified in the presence of the mutation (data not shown). Nevertheless, our results indicate that binding of SRSF1 splicing factor to ESEs present in the pseudoexon is involved in pseudoexon inclusion in the presence of the mutation because downregulation of SRSF1 induced pseudoexon skipping (Fig. 5) and an AON that targets a putative SRSF1 binding site in the pseudoexon (SRSF1 AON) restored correct splicing (Fig. 4). SRSF1 binding may be important to recognize the pseudoexon, but this event is not sufficient for pseudoexon inclusion unless the 3′ss is activated by the mutation. We have also explored the role of hnRNPA1 in pseudoexon recognition, as there is an hnRNPA1 binding site in the 3′ss that is disrupted in the presence of the mutation (Supp. Fig. S1). Pseudoexon inclusion level is not modified in wild-type minigene after transfection of SA AON or U1αCAPN3-SA, which mask hnRNPA1 binding site in the wild-type construct (Supp. Fig. S2). Besides, overexpression of hnRNPA1 did not alter the splicing pattern of exons 14 and 15 neither using wild-type nor mutant constructs (data not shown). Therefore, our results do not support a role of hnRNPA1 in pseudoexon silencing.

Therapeutic approaches based on induction of exon skipping have been applied for the correction of several mutations in many diseases in recent years [Cazzella et al., 2012; Goemans et al., 2011; Hua et al., 2011; Meyer et al., 2009; Vulin et al., 2012]. In the present study, splicing modulation has been induced for the correction of c.1782+1072G>C pseudoexon-generating deep intronic mutation in the *CAPN3* gene. Antisense sequences delivered by AONs that target pseudoexon 3′ss or 5′ss (SA AON or SD AON, respectively) induced pseudoexon skipping. However, only SD AON decreased pseudoexon inclusion levels to those observed in the presence of wild-type minigene (Fig. 2). The reason for this is unclear. These differences might reflect the accessibility of the AONs to interact with the target pre-mRNA. However, bioinformatics analysis of the sequences targeted by AONs determined that SD AON masks more putative binding sites for splicing enhancers than SA AON. Indeed, pseudoexon 5′ss has already been described as a donor site in hMp18 transcript, an isoform of *CAPN3* expressed in melanoma cells [Kawabata et al., 2003]. Therefore, we hypothesize that SD AON would restore correct splicing more efficiently by masking a potent 5′ss after a novel 3′ss created in the presence of the mutation. The accessible 5′ss would be necessary for pseudoexon recognition according to the exon definition model [Robberson et al., 1990].

Antisense sequences were also expressed from modified U-snRNAs, but they worked less efficiently than AONs (Fig. 3). Pseudoexon inclusion level with U1αCAPN3-SD, whose target sequence is identical to SD-AON, was similar to those obtained with a control U1-snRNA (Fig. 3B). As the 5′ extreme of U1αCAPN3-SD is designed to exactly target pseudoexon 5′ss, it is possible that U1αCAPN3-SD is working as a functional U1-snRNA that binds pseudoexon 5′ss and induces pseudoexon recognition by the spliceosome. Indeed, expression of modified U-snRNAs that are complementary to a mutated 5′ss can correct the exon skipping caused by these mutations [Fernandez Alanis et al., 2012]. Likewise, U7αCAPN3-SD, which also harbors SD AON sequence in its 40-mer antisense sequence, was three times less efficient than SD AON. Based on the estimation of the expression level of U-snRNAs (Fig. 3C), it is possible that U-snRNA molecule number per cell is lower than AONs, although they are expressed from their strong gene promoters. Moreover, AONs are chemically designed to be very stable molecules. U1αCAPN3-SA construct was the most effective U-snRNA molecule for pseudoexon skipping, probably because it masks more binding sites for splicing regulators than SA-AON.

Delivery of antisense sequences by AONs also restored correct splicing of endogenous *CAPN3* pre-mRNA (Fig. 6). In this case, SRSF1 AON, which targets an internal ESE in the pseudoexon, restored correct splicing more efficiently than the others. This result agrees with previously reported data where AONs targeting internal ESE motifs are more effective than those directed to splicing elements in intronic sequences [Rimessi et al., 2010]. Indeed, the AONs in clinical trials for the treatment of Duchenne Muscular Dystrophy (DMD) target internal ESE motifs in dmd exons [Arechavala-Gomeza et al., 2012].

In the mutation described here, antisense sequences induce pseudoexon skipping and therefore, restoration of full-length *CAPN3* mRNA. This would recover wild-type protein synthesis. Although control fibroblasts express *CAPN3* mRNA, we did not detect calpain 3 at the protein level (data not shown). Therefore, we are currently working to obtain an appropriate cellular model to test whether antisense sequences are able to restore calpain 3 protein expression in LGMD2A patients.

Altogether, these data demonstrate that antisense sequences expressed from modified U-snRNAs or AONs can induce the in vitro correction of the pseudoexon-generating deep intronic mutation described in this work. Modified U-snRNAs can induce long-term exon skipping when delivered to animal models from viral vectors [Denti et al., 2006; Vulin et al., 2012]. However, AONs are already in advanced phases of clinical trials [Cirak et al., 2012; Goemans et al., 2011]. Goemans et al. (2011) have recently shown that systemic administration of AONs with full-length 2′-*O*-methyl-substituted ribose moieties and phosphorothioate internucleotide linkages, the same chemistry we used in this study, results in a dose-dependent abundant expression of dystrophin in patients with DMD with no serious adverse effects. Moreover, bioinformatics analysis did not identify other human transcripts where SD and SRSF1 functional AONs would bind nonspecifically. Therefore, we consider that LGMD2A patients with c.1782+1072G>C mutation could benefit from AON treatment in the near future.

Acknowledgments

We are grateful to LGMD2A patients who participated in this study. We also wish to thank Paul Miller for editing of the manuscript, M. Huarte for giving us the control oligonucleotide and N. Razquin for technical advice.

Disclosure statement: The authors declare no conflict of interest.

References

Arechavala-Gomeza V, Anthony K, Morgan J, Muntoni F. 2012. Antisense oligonucleotide-mediated exon skipping for duchenne muscular dystrophy: progress and challenges. Curr Gene Ther 12:152–160.

Black DL. 2003. Mechanisms of alternative pre-messenger RNA splicing. Annu Rev Biochem 72:291–336.

Blazquez L, Azpitarte M, Saenz A, Goicoechea M, Otaegui D, Ferrer X, Illa I, Gutierrez-Rivas E, Vilchez JJ, Lopez de Munain A. 2008. Characterization of novel CAPN3 isoforms in white blood cells: an alternative approach for limb-girdle muscular dystrophy 2A diagnosis. Neurogenetics 9:173–182.

Blazquez L, Gonzalez-Rojas SJ, Abad A, Razquin N, Abad X, Fortes P. 2012. Increased in vivo inhibition of gene expression by combining RNA interference and U1 inhibition. Nucleic Acids Res 40:e8.

Brun C, Suter D, Pauli C, Dunant P, Lochmuller H, Burgunder JM, Schumperli D, Weis J. 2003. U7 snRNAs induce correction of mutated dystrophin pre-mRNA by exon skipping. Cell Mol Life Sci 60:557–566.

Cartegni L, Wang J, Zhu Z, Zhang MQ, Krainer AR. 2003. ESEfinder: a web resource to identify exonic splicing enhancers. Nucleic Acids Res 31:3568–3571.

Cazzella V, Martone J, Pinnaro C, Santini T, Twayana SS, Sthandier O, D'Amico A, Ricotti V, Bertini E, Muntoni F, Bozzoni I. 2012. Exon 45 skipping through U1-snRNA antisense molecules recovers the dys-nNOS pathway and muscle differentiation in human DMD myoblasts. Mol Ther 20:2134–2142.

Cirak S, Feng L, Anthony K, Arechavala-Gomeza V, Torelli S, Sewry C, Morgan JE, Muntoni F. 2012. Restoration of the dystrophin-associated glycoprotein complex after exon skipping therapy in duchenne muscular dystrophy. Mol Ther 20:462–467.

De Tullio R, Stifanese R, Salamino F, Pontremoli S, Melloni E. 2003. Characterization of a new p94-like calpain form in human lymphocytes. Biochem J 375:689–696.

Dehainault C, Michaux D, Pages-Berhouet S, Caux-Moncoutier V, Doz F, Desjardins L, Couturier J, Parent P, Stoppa-Lyonnet D, Gauthier-Villars M, Houdayer C. 2007. A deep intronic mutation in the RB1 gene leads to intronic sequence exonisation. Eur J Hum Genet 15:473–477.

Denti MA, Rosa A, D'Antona G, Sthandier O, De Angelis FG, Nicoletti C, Allocca M, Pansarasa O, Parente V, Musaro A, Auricchio A, Bottinelli R, et al. 2006. Chimeric adeno-associated virus/antisense U1 small nuclear RNA effectively rescues dystrophin synthesis and muscle function by local treatment of mdx mice. Hum Gene Ther 17:565–574.

Desmet FO, Hamroun D, Lalande M, Collod-Beroud G, Claustres M, Beroud C. 2009. Human splicing finder: an online bioinformatics tool to predict splicing signals. Nucleic Acids Res 37:e67.

Ermolova N, Kudryashova E, DiFranco M, Vergara J, Kramerova I, Spencer MJ. 2011. Pathogenity of some limb girdle muscular dystrophy mutations can result from reduced anchorage to myofibrils and altered stability of calpain 3. Hum Mol Genet 20:3331–3345.

Fardeau M, Eymard B, Mignard C, Tome FM, Richard I, Beckmann JS. 1996. Chromosome 15-linked limb-girdle muscular dystrophy: clinical phenotypes in reunion island and french metropolitan communities. Neuromuscul Disord 6:447–453.

Fernandez Alanis E, Pinotti M, Dal Mas A, Balestra D, Cavallari N, Rogalska ME, Bernardi F, Pagani F. 2012. An exon-specific U1 small nuclear RNA (snRNA) strategy to correct splicing defects. Hum Mol Genet 21:2389–2398.

Fortes P, Cuevas Y, Guan F, Liu P, Pentlicky S, Jung SP, Martinez-Chantar ML, Prieto J, Rowe D, Gunderson SI. 2003. Inhibiting expression of specific genes in mammalian cells with 5' end-mutated U1 small nuclear RNAs targeted to terminal exons of pre-mRNA. Proc Natl Acad Sci U S A 100:8264–8269.

Friedman KJ, Kole J, Cohn JA, Knowles MR, Silverman LM, Kole R. 1999. Correction of aberrant splicing of the cystic fibrosis transmembrane conductance regulator (CFTR) gene by antisense oligonucleotides. J Biol Chem 274:36193–36199.

Gedicke-Hornung C, Behrens-Gawlik V, Reischmann S, Geertz B, Stimpel D, Weinberger F, Schlossarek S, Precigout G, Braren I, Eschenhagen T, Mearini G, Lorain S, et al. 2013. Rescue of cardiomyopathy through U7snRNA-mediated exon skipping in Mybpc3-targeted knock-in mice. EMBO Mol Med 5:1128–1145.

Goemans NM, Tulinius M, van den Akker JT, Burm BE, Ekhart PF, Heuvelmans N, Holling T, Janson AA, Platenburg GJ, Sipkens JA, Sitsen JM, Aartsma-Rus A, et al. 2011. Systemic administration of PRO051 in Duchenne's muscular dystrophy. N Engl J Med 364:1513–1522.

Goren A, Ram O, Amit M, Keren H, Lev-Maor G, Vig I, Pupko T, Ast G. 2006. Comparative analysis identifies exonic splicing regulatory sequences—the complex definition of enhancers and silencers. Mol Cell 22:769–781.

Goyenvalle A, Vulin A, Fougerousse F, Leturcq F, Kaplan JC, Garcia L, Danos O. 2004. Rescue of dystrophic muscle through U7 snRNA-mediated exon skipping. Science 306:1796–1799.

Homolova K, Zavadakova P, Doktor TK, Schroeder LD, Kozich V, Andresen BS. 2010. The deep intronic c.903+469T>C mutation in the MTRR gene creates an SF2/ASF binding exonic splicing enhancer, which leads to pseudoexon activation and causes the cblE type of homocystinuria. Hum Mutat 31:437–444.

Hua Y, Sahashi K, Hung G, Rigo F, Passini MA, Bennett CF, Krainer AR. 2010. Antisense correction of SMN2 splicing in the CNS rescues necrosis in a type III SMA mouse model. Genes Dev 24:1634–1644.

Hua Y, Sahashi K, Rigo F, Hung G, Horev G, Bennett CF, Krainer AR. 2011. Peripheral SMN restoration is essential for long-term rescue of a severe spinal muscular atrophy mouse model. Nature 478:123–126.

Incitti T, De Angelis FG, Cazzella V, Sthandier O, Pinnaro C, Legnini I, Bozzoni I. 2010. Exon skipping and duchenne muscular dystrophy therapy: selection of the most active U1 snRNA antisense able to induce dystrophin exon 51 skipping. Mol Ther 18:1675–1682.

Kawabata Y, Hata S, Ono Y, Ito Y, Suzuki K, Abe K, Sorimachi H. 2003. Newly identified exons encoding novel variants of p94/calpain 3 are expressed ubiquitously and overlap the alpha-glucosidase C gene. FEBS Lett 555:623–630.

Krahn M, Pecheux C, Chapon F, Beroud C, Drouin-Garraud V, Laforet P, Romero NB, Penisson-Besnier I, Bernard R, Urtizberea JA, Leturcq F, Levy N. 2007. Transcriptional explorations of CAPN3 identify novel splicing mutations, a large-sized genomic deletion and evidence for messenger RNA decay. Clin Genet 72:582–592.

Kramerova I, Kudryashova E, Ermolova N, Saenz A, Jaka O, Lopez de Munain A, Spencer MJ. 2012. Impaired calcium calmodulin kinase signaling and muscle adaptation response in the absence of calpain 3. Hum Mol Genet 21:3193–3204.

Kramerova I, Kudryashova E, Wu B, Ottenheijm C, Granzier H, Spencer MJ. 2008. Novel role of calpain-3 in the triad-associated protein complex regulating calcium release in skeletal muscle. Hum Mol Genet 17:3271–3280.

Mancini C, Vaula G, Scalzitti L, Cavalieri S, Bertini E, Aiello C, Lucchini C, Gatti RA, Brussino A, Brusco A. 2012. Megalencephalic leukoencephalopathy with subcortical cysts type 1 (MLC1) due to a homozygous deep intronic splicing mutation (c.895-226T>G) abrogated in vitro using an antisense morpholino oligonucleotide. Neurogenetics 13:205–214.

Meyer K, Marquis J, Trub J, Nlend Nlend R, Verp S, Ruepp MD, Imboden H, Barde I, Trono D, Schumperli D. 2009. Rescue of a severe mouse model for spinal muscular atrophy by U7 snRNA-mediated splicing modulation. Hum Mol Genet 18:546–555.

Milic A, Daniele N, Lochmuller H, Mora M, Comi GP, Moggio M, Noulet F, Walter MC, Morandi L, Poupiot J, Roudaut C, Bittner RE, Bartoli M, Richard I. 2007. A third of LGMD2A biopsies have normal calpain 3 proteolytic activity as determined by an in vitro assay. Neuromuscul Disord 17:148–156.

Nascimbeni AC, Fanin M, Tasca E, Angelini C. 2010. Transcriptional and translational effects of intronic CAPN3 gene mutations. Hum Mutat 31:E1658–E1669.

Ojima K, Ono Y, Ottenheijm C, Hata S, Suzuki H, Granzier H, Sorimachi H. 2011. Non-proteolytic functions of calpain-3 in sarcoplasmic reticulum in skeletal muscles. J Mol Biol 407:439–449.

Pinotti M, Rizzotto L, Balestra D, Lewandowska MA, Cavallari N, Marchetti G, Bernardi F, Pagani F. 2008. U1-snRNA-mediated rescue of mRNA processing in severe factor VII deficiency. Blood 111:2681–2684.

Richard I, Broux O, Allamand V, Fougerousse F, Chiannilkulchai N, Bourg N, Brenguier L, Devaud C, Pasturaud P, Roudaut C. 1995. Mutations in the proteolytic enzyme calpain 3 cause limb-girdle muscular dystrophy type 2A. Cell 81:27–40.

Rimessi P, Fabris M, Bovolenta M, Bassi E, Falzarano S, Gualandi F, Rapezzi C, Coccolo F, Perrone D, Medici A, Ferlini A. 2010. Antisense modulation of both exonic and intronic splicing motifs induces skipping of a DMD pseudo-exon responsible for x-linked dilated cardiomyopathy. Hum Gene Ther 21:1137–1146.

Robberson BL, Cote GJ, Berget SM. 1990. Exon definition may facilitate splice site selection in RNAs with multiple exons. Mol Cell Biol 10:84–94.

Rodriguez-Pascau L, Coll MJ, Vilageliu L, Grinberg D. 2009. Antisense oligonucleotide treatment for a pseudoexon-generating mutation in the NPC1 gene causing niemann-pick type C disease. Hum Mutat 30:E993–E1001.

Schmid F, Glaus E, Barthelmes D, Fliegauf M, Gaspar H, Nurnberg G, Nurnberg P, Omran H, Berger W, Neidhardt J. 2011. U1 snRNA-mediated gene therapeutic correction of splice defects caused by an exceptionally mild BBS mutation. Hum Mutat 32:815–824.

Schumperli D, Pillai RS. 2004. The special sm core structure of the U7 snRNP: far-reaching significance of a small nuclear ribonucleoprotein. Cell Mol Life Sci 61:2560–2570.

Smith PJ, Zhang C, Wang J, Chew SL, Zhang MQ, Krainer AR. 2006. An increased specificity score matrix for the prediction of SF2/ASF-specific exonic splicing enhancers. Hum Mol Genet 15:2490–2508.

Sorimachi H, Imajoh-Ohmi S, Emori Y, Kawasaki H, Ohno S, Minami Y, Suzuki K. 1989. Molecular cloning of a novel mammalian calcium-dependent protease distinct from both m- and mu-types. specific expression of the mRNA in skeletal muscle. J Biol Chem 264:20106–20111.

Spier I, Horpaopan S, Vogt S, Uhlhaas S, Morak M, Stienen D, Draaken M, Ludwig M, Holinski-Feder E, Nothen MM, Hoffmann P, Aretz S. 2012. Deep intronic APC mutations explain a substantial proportion of patients with familial or early-onset adenomatous polyposis. Hum Mutat 33:1045–1050.

Stamm S, Riethoven JJ, Le Texier V, Gopalakrishnan C, Kumanduri V, Tang Y, Barbosa-Morais NL, Thanaraj TA. 2006. ASD: a bioinformatics resource on alternative splicing. Nucleic Acids Res 34:D46–D55.

Tanner G, Glaus E, Barthelmes D, Ader M, Fleischhauer J, Pagani F, Berger W, Neidhardt J. 2009. Therapeutic strategy to rescue mutation-induced exon skipping in rhodopsin by adaptation of U1 snRNA. Hum Mutat 30:255–263.

Urtasun M, Saenz A, Roudaut C, Poza JJ, Urtizberea JA, Cobo AM, Richard I, Garcia Bragado F, Leturcq F, Kaplan JC, Marti Masso JF, Beckmann JS, Lopez de Munain A. 1998. Limb-girdle muscular dystrophy in guipuzcoa (basque country, spain). Brain 121 (Pt 9):1735–1747.

van Deutekom JC, Bremmer-Bout M, Janson AA, Ginjaar IB, Baas F, den Dunnen JT, van Ommen GJ. 2001. Antisense-induced exon skipping restores dystrophin expression in DMD patient derived muscle cells. Hum Mol Genet 10:1547–1554.

Vulin A, Barthelemy I, Goyenvalle A, Thibaud JL, Beley C, Griffith G, Benchaouir R, le Hir M, Unterfinger Y, Lorain S, Dreyfus P, Voit T, Carlier P, Blot S, Garcia L. 2012. Muscle function recovery in golden retriever muscular dystrophy after AAV1-U7 exon skipping. Mol Ther 20:2120–2133.

Wein N, Avril A, Bartoli M, Beley C, Chaouch S, Laforet P, Behin A, Butler-Browne G, Mouly V, Krahn M, Garcia L, Levy N. 2010. Efficient bypass of mutations in dysferlin deficient patient cells by antisense-induced exon skipping. Hum Mutat 31:136–142.

Will CL, Luhrmann R. 2011. Spliceosome structure and function. Cold Spring Harb Perspect Biol 3(7):a003707.